Available online at www.sciencedirect.com
SCIENCE DIRECT®
Polymer 45 (2004) 2261–2269
polymer
www.elsevier.com/locate/polymer

Star polymers via atom transfer radical polymerization from adamantane-based cores

Chih-Feng Huang[a], Hsin-Fang Lee[a], Shiao-Wei Kuo[a], Hongyao Xu[a,b], Feng-Chih Chang[a,*]

[a]*Department of Applied Chemistry, National Chiao Tung University, Hsin Chu, Taiwan, ROC*
[b]*Department of Chemistry, Anhui University, Anhui 230039, China*

Received 14 October 2003; received in revised form 14 January 2004; accepted 28 January 2004

Abstract

A series of novel multifunctional initiators derived from adamantane-based derivatives have been used in the syntheses of various styrenic and (meth)acrylic star polymers by atom transfer radical polymerization (ATRP). Conditions were identified in each system to produce star polymers with nearly monomodal molecular distributions. These synthesized star polymers have glass transition temperatures similar to those known for high-molecular-weight linear polymers. We obtained a series of adamantane-contained star polymers covering a wide range of molecular weights by adjusting the monomer-to-initiator ratio and the solvent polarity. Because of reaction heterogeneity and inevitable termination processes, the occurrence of star–star coupling led to a lower than predicted molecular weight polydispersity. When hydrolyzed from their cores by NaOH, the values of M_w of the arms of the PMMA star polymer did not change with reaction time, at least for the first 48 h of the reaction, which implies that no significant PMMA hydrolysis occurs within this interval of time.
© 2004 Elsevier Ltd. All rights reserved.

Keywords: Adamantane; Atom transfer radical polymerization; PMMA

1. Introduction

The synthesis and characterization of star polymers continue to be the areas of exploration in the pursuit of structure–property relationships in macromolecular science [1]. Star polymers have attracted great interest, especially from the viewpoints of their rheological and physical properties and their potential applications [2–4]. Methods for making star polymers fall into two broad classes. In the 'arm first' approach, monofunctional living linear macromolecules are synthesized initially. Star formation then occurs in one of two ways: a difunctional co-monomer is used to provide cross-linking through propagation [5] or a multifunctional terminating agent is added connecting a precise number of arms to a central core molecule. In the first case, the microgel technique can be used to produce macromolecules with a large number of arms. In the second case, separation techniques are used to isolate star polymers from uncoupled linear polymers. The second method for synthesizing star polymers is the 'core first' approach. Multifunctional initiators are used to grow chains from a central core resulting in macromolecules with well-defined structures in terms of both the number and length of the arms. Furthermore, the reaction product consists solely of star polymers—there is an absence of linear polymers. In many cases, however, the multifunctional initiators must be presynthesized and, in addition, only a limited number of studies have used this method because of the poor solubility of the multiply charged species needed to initiate ionic polymerizations [6–10].

An efficient method for the synthesis of star polymers is living polymerization, and there are at least three variations of this approach: (1) living polymerization with a multifunctional initiator, (2) coupling reactions of linear living polymers with a multifunctional coupling agent, and (3) linking reactions of linear living polymers with a divinyl compound (linking agent). Many 'living' systems are known and they encompass many polymerization mechanisms, such as anionic, cationic, radical, ring-opening and coordinative processes. To date, most star polymers have been synthesized by ionic processes [11–15]. Increasingly, the synthesis by living radical polymerization has gained interest, however, because it is tolerant of impurities,

* Corresponding author. Tel.: +886-3-5727077; fax: +886-3-5719507.
E-mail address: changfc@cc.nctu.edu.tw (F.C. Chang).

0032-3861/$ - see front matter © 2004 Elsevier Ltd. All rights reserved.
doi:10.1016/j.polymer.2004.01.051

adventitious water, and high temperatures and can be employed for a wide variety of various vinylic monomers. In the past decade, significant efforts have been devoted to the development of living/controlled polymerization based on free radical chemistry [16]. Three main approaches have been developed: the first involves the mediation of the controlled free radical procedure by stable free radical polymerization (SFRP) [17], and the second, reversible addition–fragmentation transfer polymerization (RAFT) [18], while the third, atom transfer radical polymerization (ATRP) [19]. In these approaches, the free radicals are generated either by a thermal process (SFRP), a catalyzed reaction (ATRP), or reversibly by a degenerative exchange process with dormant species (RAFT). Atom-transfer radical polymerization, which evolved from the Kharasch reaction and is mediated by a variety of metal complexes, is one of the most widely used controlled radical polymerization techniques. The process was discovered independently by Matyjaszewski [20,21] and Sawamoto [22] et al., and its mechanism has been thoroughly investigated. The ATRP process uses a halide, as an initiator, and a metal atom, with complexing ligands, in a low oxidation state [23–27]. The process involves the successive transfer of the halide from the dormant polymer chain to the ligated metal complex, forming a dynamic equilibrium between active and dormant species. ATRP has proven to be a powerful tool in the synthesis of polymers with narrow polydispersity (PDI < 1.5) and controlled molecular weight.

Our interest in star polymers was stimulated by the reports of Menger et al. [28–30], in which geminis surfactants were synthesized featuring multiple arms containing α-haloester, units, potential initiators for atom transfer radical polymerization. We have extended this synthetic route to the preparation of starlike polymers from the thermodynamically stable, rigid core of adamantane. In this paper we report the synthesis of multiarm initiators and discuss their application in ATRP procedures, based on a general core-first approach, for the synthesis of star polymers with well-defined structures.

2. Experimental

2.1. Materials

Styrene was distilled from calcium hydride before use. Methyl methacrylate, *tert*-butyl acrylate, and *n*-butyl acrylate were all rinsed three times with 5% sodium hydroxide solution and once with water. After drying with magnesium sulfate, these monomers were purified by distillation from calcium chloride. Following purification, all monomers were stored in a freezer. Triethylamine was stirred over magnesium sulfate and filtered prior to use. Copper(I) bromide (CuBr) was stirred in glacial acetic acid overnight, filtered, and then rinsed with absolute ethanol under a blanket of argon and dried under vacuum at 60 °C overnight. All solvents were distilled prior to use. Merck Kieselgel 60 (230–400 mesh) was used for flash chromatography on silica gel. 4-Dimethylaminopyridine (DMAP), Amberlite IR-120 (H form) cation exchange resin, *N*,*N*,*N*′,*N*″,*N*‴-pentamethyldiethylenetriamine (PMDETA), 4,4′-dinonyl-2,2′-dipyridyl (dNBipy), bromoacetyl bromide, 2-bromopropionyl bromide, and 4-vinylbenzyl chloride were used as received.

2.2.1. 1,3,5,7-Tetrabromoadamantane (**2**)

The tetrabromide was prepared by modifying of a reported procedure [11]. Adamantane (**1**) (4.86 g, 35.75 mmol) was added in small portions over 30 min to a stirred mixture of bromine (22.5 ml) and anhydrous aluminum chloride (5 g, 37.5 mmol) at 0 °C. The mixture was then slowly heated to 70 °C and held at that temperature for 24 h. Hydrogen bromide evolved vigorously during the addition and heating. The reaction mixture was treated subsequently with aqueous sodium sulfite and hydrochloric acid. The resulting solid was filtered, dried in vacuum, and recrystallized from CH_3CN to give 10.10 g (63%) of tan crystals (10.10 g, 63%); mp 246–248 °C (lit. [11] 245–247 °C); ^{1}H NMR ($CDCl_3$) $\delta = 2.71$ (s, 12H) ppm; ^{13}C NMR ($CDCl_3$) $\delta = 55.0$, 54.8 ppm. Anal. Calcd for $C_{10}H_{12}Br_4$: C, 26.58; H, 2.68. Found: C, 26.66; H, 2.68.

2.2.2. 1,3,5,7-Tetrahydroxyadamantane (**3**)

The tetraalcohol was prepared by modifying a published procedure [12]. 1,3,5,7-Tetrabromoadamantane (8.34 g, 18.44 mmol) and Ag_2SO_4 (12.76 g, 40.90 mmol) were suspended in concentrated sulfuric acid (20 ml) and the mixture was slowly heated to 80 °C and stirred at that temperature for 7 h. After cooling, the AgBr precipitate was removed by filtration and the solution was rinsed with water. The filtrate was neutralized with KOH and evaporated. The resulting gray residue was dried and then extracted overnight with ethanol in a Soxhlet apparatus. After evaporation of the ethanol, the residue was dissolved in methanol and filtered. Recrystallization from MeOH/EtOH/acetone yielded a white solid (2.88 g, 78%); mp 316–318 °C (lit. [12] 317–320 °C); ^{1}H NMR (DMSO-d_6) $\delta = 4.58$ (s, 4H), 1.36 (s, 12H) ppm; ^{13}C NMR (DMSO-d_6) $\delta = 68.9$, 51.5 ppm. Anal. Calcd for $C_{10}H_{16}O_4$: C, 59.98; H, 8.05. Found: C, 59.92; H, 8.11.

2.2.3. 1,3,5,7-Tetrakis(bromoacetoxy)adamantane (**4**, *AdAcBr*)

4-(Dimethylamino)pyridine (DMAP, 20 mg) was added into a stirred suspension of 1,3,5,7-tetrahydroxyadamantane (1.18 g, 5.9 mmol) in pyridine (1.9 ml, 23.6 mmol) and CH_3CN (12 ml). Bromoacetyl bromide (4.12 ml, 47.2 mmol) was then added dropwise at 0 °C over 1 h. The ice bath was removed and stirring was continued at 50 °C for 5 h, after which time the solution became transparent and homogeneous. Hydrochloric acid (6 M, 6 ml) and CH_2Cl_2 were then added to the reaction mixture.

The aqueous layer was extracted with CH_2Cl_2 (2 × 10 ml), and the combined organic layers were concentrated to give a light-brown solid residue. The solid was dissolved in CH_2Cl_2 (5 ml) and washed sequentially with brine and aqueous Na_2CO_3 (0.5 M, 5 ml), during which the organic layer turned brown-black in color. This layer was concentrated and purified by passing through a silica gel column. Elution with CH_2Cl_2 gave the desired product as a yellow-white solid, which was recrystallized from CH_3CN/MeOH/H_2O to afford white needles (2.48 g, 70%); mp 169–171 °C; ^{1}H NMR ($CDCl_3$) $\delta = 3.76$ (s, 8H), 2.58 (s, 12H) ppm; ^{13}C NMR ($CDCl_3$) $\delta = 166.0$, 79.4, 42.8, 26.6 ppm. Anal. Calcd for $C_{18}H_{20}Br_4O_8$: C, 31.61; H, 2.95. Found: C, 32.01; H, 3.20.

2.2.4. 1,3,5,7-Tetrakis(bromopropionyloxy)adamantane (*5*, *AdPpBr*)

5 was prepared by a similar experimental procedure as described for **4**, expect that 2-bromopropionyl bromide was used in place of bromoacetyl bromide. Yield: 65% (light-yellow needles); mp = 229–231 °C; ^{1}H NMR ($CDCl_3$) $\delta = 1.75$ (d, 12H), 2.56 (s, 12H), 4.24 (q, 4H) ppm; ^{13}C NMR ($CDCl_3$) $\delta = 168.8$, 78.8, 42.4, 40.6, 21.3 ppm. Anal. Calcd for $C_{22}H_{28}Br_4O_8$: C, 35.70; H, 3.81. Found: C, 35.84; H, 3.96.

2.2.5. 1,3,5,7-Tetrakis(4-chloromethylphenyl)adamantane (*6*, *AdPhCl*)

In a 50 ml round-bottom flask, the sample of 1,3,5,7-tetrahydroxyadamantane (**3**) (1.5 g) was dissolved in dry $CHCl_3$ (25 ml) along with triethylamine (1.5 ml). A $CHCl_3$ solution of 4-(chloromethyl)benzoyl chloride (3.5 g in 4 ml $CHCl_3$) was added dropwisely at 0 °C over a period of 40 min. After stirring for 24 h at room temperature, the mixture was extracted with CH_2Cl_2 (2 × 10 ml), and the combined organic layers were concentrated to give a light-yellow solid residue. The solid was dissolved in 5 ml of CH_2Cl_2 and washed with brine and with 5 ml of aqueous 0.5 M Na_2CO_3, after which the organic layer turned transparent. This organic layer was concentrated and purified by filtering through a silica gel column. Elution with CH_2Cl_2 gave the desired product as a white solid, which was recrystallized from CH_3CN/MeOH system afforded white needles yielding 6.0 g (72%) with mp = 180–182 °C; ^{1}H NMR ($CDCl_3$) δ (ppm) = 8.18(d, 8H), 7.60(d, 8H), 4.65 (s, 8H), 2.59 (s, 12H); ^{13}C NMR ($CDCl_3$) δ (ppm) = 167.0, 145.1, 130.8, 129.9, 128.7, 80.4, 42.6, 28.6. Anal. Calcd for $C_{42}H_{36}Cl_4O_8$: C, 62.24; H, 4.48. Found: C, 62.14; H, 4.32.

2.2. General procedure for synthesis of star polymers by ATRP

A typical polymerization is as follows: CuBr (0.4 mmol) was placed into a dry 25 ml round-bottom flask equipped with a stirrer bar. Deoxygenated solvent (10 ml), monomer (40 mmol) and ligand (0.4 mmol) were added sequentially and the solution was stirred for 20 min to form the Cu complex. The initiator (0.1 mmol) was then added. This whole process took place in a nitrogen-filled dry box. An aliquot of the solution (ca. 0.1 ml) was removed and then polymerization was carried out on the bulk sample at the appropriate temperature in an oil bath. The reaction mixture turned dark green immediately and became progressively more viscous. Periodically, aliquots (0.1 ml) were removed for analysis. Exotherms of 2–4 °C were typically observed, indicating that polymerization was occurring. Upon completion of the reaction, the mixture was diluted five-fold with tetrahydrofuran (THF) and stirred with of Amberlite IR-120 (H form) cation-exchange resin (3–5 g) for 30–60 min to remove the catalyst. The mixture was then passed through an alumina column and precipitated into 10% H_2O/methanol (500 ml). This purification protocol resulted in the loss of up to ~10% of the polymer as a result of adsorption. The resulting polymers were filtered and dried overnight at 60 °C under vacuum.

2.3. Measurements

Molecular weights and molecular weight distributions were determined by gel permeation chromatography (GPC) using a Waters 510 HPLC—equipped with a 410 Differential Refractometer, a UV detector, and three Ultrastyragel columns (100, 500, and 10^3 Å) connected in series in order of increasing pore size—using THF as an eluent at a flow rate of 0.4 ml/min. The molecular weight calibration curve was obtained using polystyrene standards. Thermal analysis was carried out on a DSC instrument (DuPont model 910 DSC-9000 Controller) with a scan rate of 20 °C/min and temperature range of 30–250 °C under a nitrogen atmosphere. The sample (ca. 5–10 mg) was weighed and sealed in an aluminum pan. The sample was cooled rapidly to room temperature from the first scan and then up to 250 °C at a scan rate of 20 °C/min. The glass transition temperature is taken as the midpoint of the heat capacity transition between the upper and lower points of deviation from the extrapolated glass and liquid lines. FTIR spectroscopy measurements were made from an NaCl disk using a Nicolet Avatar 320 FT-IR Spectrometer, with 32 scans collected at a resolution of 1 cm^{-1}. A THF solution containing the sample was cast onto an NaCl disk and dried under conditions similar to those used in the bulk preparation. The sample chamber was purged with nitrogen to maintain the film's dryness. ^{1}H NMR spectra were recorded in $CDCl_3$ on a Bruker AM 500 (500 MHz) spectrometer, with the solvent signal as an internal standard. ^{13}C NMR spectra were recorded in $CDCl_3$ at 125 MHz on a Bruker AM 500 spectrometer with the carbon signal serving as the internal standard. Elemental analysis was carried out on a Heraus CHN-Rapid Elemental Analyzer.

3. Results and discussion

The ATRP initiators AdAcBr **4**, AdPpBr **5** and AdPhCl **6** were prepared from the tetrahydroxy-functionalized adamantane derivative **3**, whose synthesis has been described previously [29,30]. Acylation of tetrahydroxyadamantane with acid bromides or acid chlorides in the presence of pyridine afforded the adamantane-based initiators (Scheme 1). Fig. 1 depicts ^{1}H NMR spectra of the initiators **4**, **5** and **6** with assignments for all of the peaks. These tetrahedral initiators are soluble in most common organic solvents, such as chloroform, benzene, toluene or acetonitrile, resulting in homogeneous dispersions during polymerization. Adamantane derivatives containing activated halide end groups are necessary for initiation of the ATRP process. These star polymers are noteworthy for the rigid tetrahedral disposition of their chain origins because of the geometry of the adamantane core. ATRP is often described as a living/controlled radical polymerization because the irreversible termination reactions that consume radicals are suppressed on account of a very low radical concentration (Scheme 2). These low concentrations of radicals occur because deactivation is much faster than activation. Table 1 lists reaction conditions, yields, molecular weights, and values of T_g for the products of star polymerization using the adamantane-based initiators. Many monomers—styrene, acrylates, and methacrylates—have been reported so far

Table 1
Reaction conditions (CuBr catalyst; *N,N,N′,N″,N‴*-pentamethyldiethylenetriamine ligand; nitrogen atmosphere; mole ratio of monomer/initiators, 400:1) for the synthesis of star polymers from adamantane-based initiators

Initiator[a]	Monomer[b]	T (°C)	Time (h)	Yield (%)	M_w (GPC)[c]	PDI[d]	T_g (°C)
4	MMA	90	24	5	2800	1.15	79
5	MMA	90	8	70	28,740	1.18	102
5	*t*BA	80	7	80	32,740	1.22	46
5	S	110	4	46	19,140	1.30	101
6	MMA	90	16	51	21,210	1.25	100
6	S	110	5	35	14,810	1.26	102

[a] Initiators: **4** = 1,3,5,7-tetrakis(bromoacetoxy)adamantane; **5** = 1,3,5,7-tetrakis(bromopropionyloxy)adamantane; **6** = 1,3,5,7-tetrakis(4-chloromethylphenyl)adamantane.
[b] Monomers: S = styrene; MMA = methyl methacrylate; *t*BA = *tert*-butyl methacrylate.
[c] Weight-average molar mass from GPC traces.
[d] Polydispersity index from GPC traces using refractometric detection.

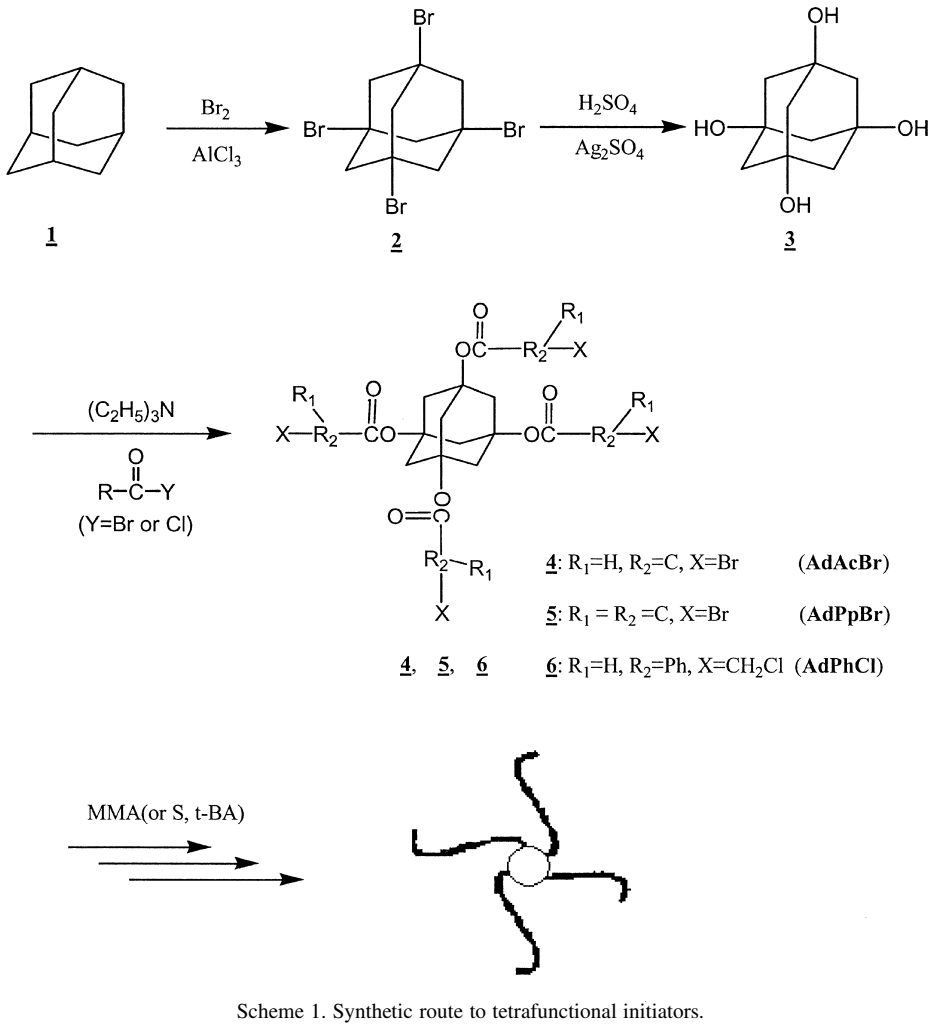

Scheme 1. Synthetic route to tetrafunctional initiators.

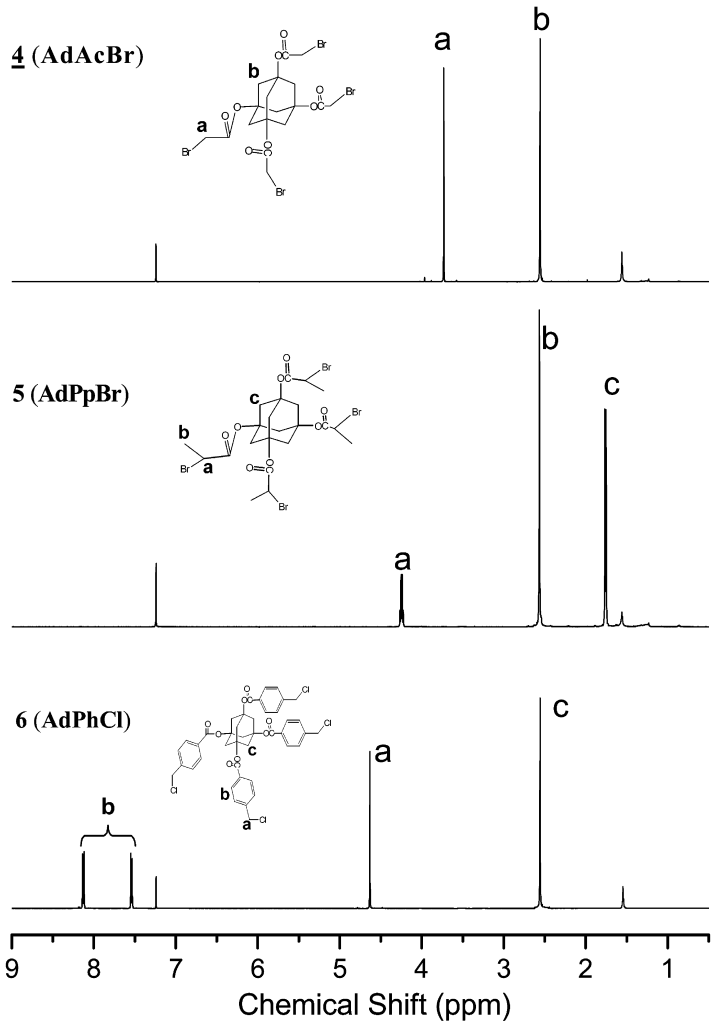

Fig. 1. ^{1}H NMR spectra of initiators **4**, **5**, and **6** in $CDCl_3$.

for ATRP polymerizations. DSC measurements show that the star polymers undergo a glass transition (T_g) at temperatures similar to those of known high-molecular-weight linear polymers. Table 1 lists the values of T_g determined for the different star polymers synthesized. Above their values of T_g, these star polymers are easily processable.

In a typical ATRP, the concentrations of the active species remain unchanged throughout the reaction, which is a feature that can be verified by a linear semilogarithmic plot of monomer conversion versus time, as shown in Fig. 2. Fig. 2(b) shows that the MMA in toluene deviated from the linear relationship after a reaction time of 4 h, which we interpret as indicating the occurrence of termination reactions through star–star coupling. As this termination reaction occurs, the number of active sites decreases, which results in a decrease in the rate of polymerization. In addition, a portion of the original CuX catalyst becomes deactivated, through oxidization into CuX_2, which results in the elimination of some active sites. Due to such 'catalyst poisoning', the maximum monomer conversion is ~78% when the toluene is employed as solvent as shown in Fig. 2(b). Solvent effect is observed by comparing Fig. 2(a) and (b). Increasing the polarity of the solvent increases solubility of the Cu(I)Br/ligand complex [31,32] promoting the homogeneous processes of ATRP and results in a well controlled linear semilogarithmic relation of monomer conversion versus time as shown in Fig. 2(a). Table 2 summarized results of ATRP process with different reaction media.

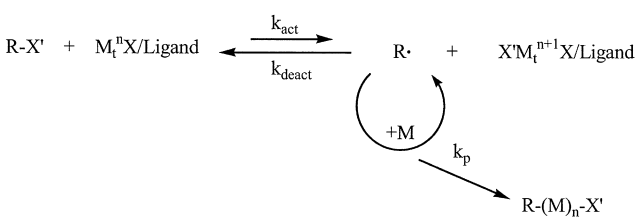

Scheme 2. Dynamic equilibrium that exists between the propagating and dormant species when a metal complex is used as the reversible halogen atom transfer reagent.

The rate of polymerization in ATRP depends on the

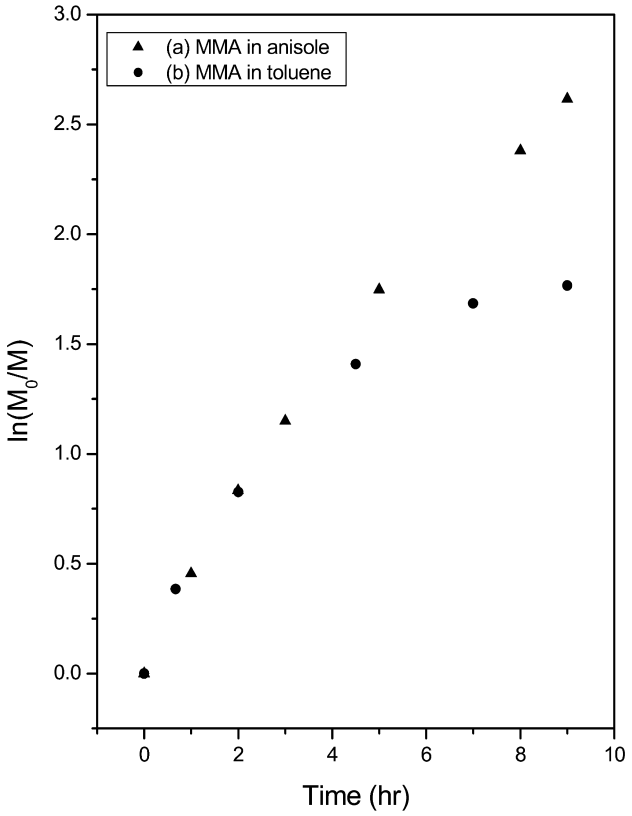

Fig. 2. Semilogarithmic kinetic plot for ATRP with various of monomers at 90 °C [conditions: monomer (4 M), solvent (toluene or anisole), CuBr as catalyst, *N*,*N*,*N*′,*N*″,*N*″-pentamethyldiethylenetriamine as ligand, molar ratio of [I]:[C]:[L] = 1:1:1, initiated by **5**].

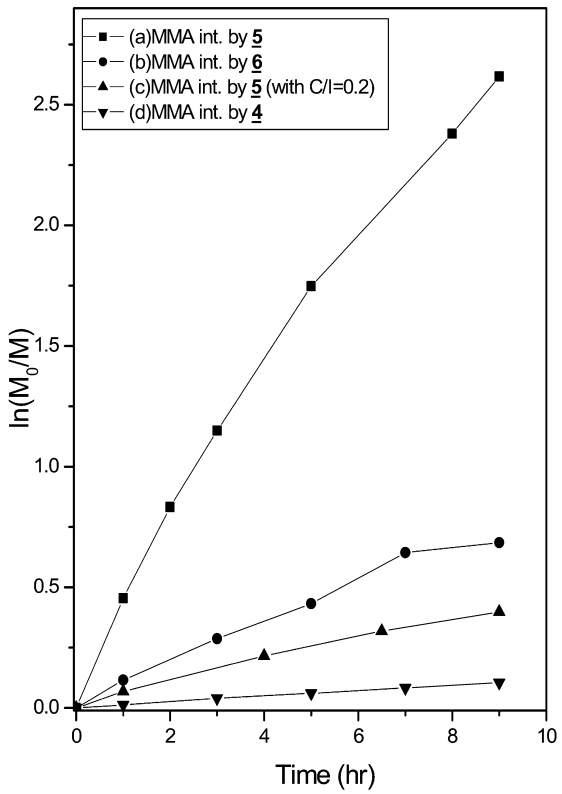

Fig. 3. Semilogarithmic kinetic plot for the ATRP of MMA monomer with various initiators at 90 °C [conditions: monomer (4 M), anisole, CuBr catalyst, *N*,*N*,*N*′,*N*″,*N*″-pentamethyldiethylenetriamine ligand].

concentration of the propagating radicals, the initiator efficiency, and the concentration of the deactivator in the system (e.g., Cu(II) halides) [33]. The rate of ATRP for the MMA monomer in the AdPhCl/CuX system, as shown in Fig. 3(b), is rather slow, which is a situation that is probably caused by the poor initiation efficiency that results in smaller amounts of both propagating radicals and Cu(II) species than those in the AdPpBr/CuX system, shown in Fig. 3(a). It has been reported that the phenylethyl halide functional group is a poor initiator for the polymerization of MMA [34]. An initiator structure that is similar to the structure of the dormant polymer species is more favorable in initiating polymerization. Consequently, we believe that the dissimilar structure of the AdPhCl/CuX system results in the lower efficiency of the MMA initiation. The rate of polymerization initiated by AdAcBr **4** (Fig. 3(d)) is the slowest among all initiators. The AdAcBr **4** lacks an inductively or resonance-stabilizing substituent that is necessary for an efficient initiator of ATRP.

GPC is a useful technique for determining the average molecular weight of the star polymer and provides information on the structural integrity of the molecule. Fig. 4 shows GPC traces of star polymers synthesized at 90 °C in toluene at different time intervals. The presence of high-molecular-weight species derived from star–star coupling can be observed in these GPC traces. For the

Table 2
Atom transfer radical polymerization (CuBr catalyst; nitrogen atmosphere) using initiator **5**

Monomer[a]	Ligand[b]	I:C:L[c]	Solvent	Time (h)	Yield (%)	M_w (GPC)[d]	PDI
MMA	PMDETA	1:1:1	Bulk	4	45	24,740	1.30(bimodal)
MMA	PMDETA	1:1:1	Toluene	8	63	31,940	1.27(bimodal)
MMA	PMDETA	1:1:1	Anisole	3	35	20,740	1.20
MMA	dNBipy	1:1:1	Toluene	4	50	26,740	1.22
MMA	PMDETA	1:0.2:0.2	Toluene	8	40	22,740	1.18

[a] Monomers: MMA = methyl methacrylate.
[b] Ligand: PMDETA = *N*,*N*,*N*′,*N*″,*N*″-pentamethyldiethylenetriamine; dNBipy = 4,4′-dinonyl-2,2′-dipyridyl.
[c] Mole ratio of initiator to copper bromide to ligand.
[d] Polydispersity index from GPC traces using refractometric detection.

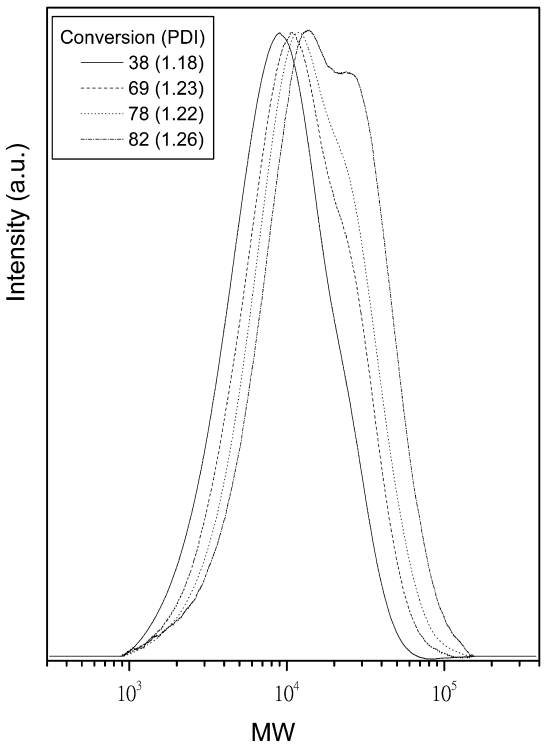

Fig. 4. GPC traces of star polymers obtained from the experiment at 90 °C. Conditions: MMA monomer (4 M), toluene, CuBr catalyst, *N*,*N*,*N*′,*N*″,*N*″-pentamethyldiethylenetriamine ligand.

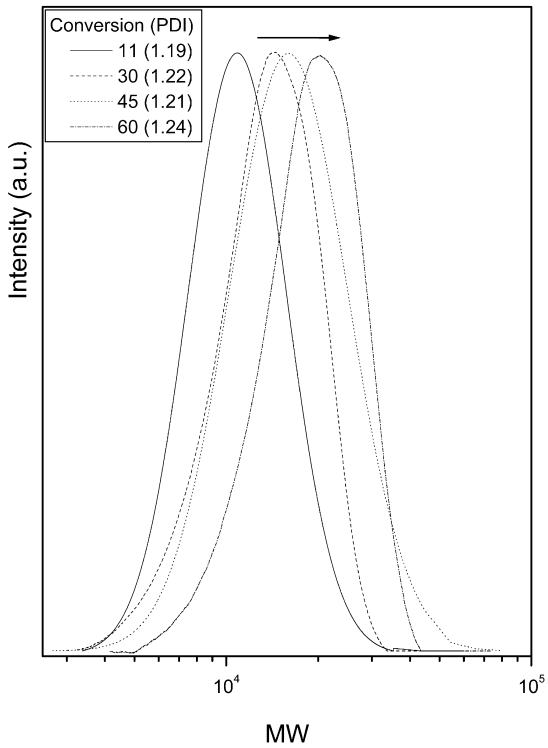

Fig. 5. GPC traces of star polymers obtained from the experiment at 90 °C. Conditions: MMA monomer (4 M), anisole, CuBr catalyst, *N*,*N*,*N*′,*N*″,*N*″-pentamethyldiethylenetriamine ligand, molar ratio of [I]:[C]:[L] = 1:0.2:0.2.

reason mentioned above, under these specific conditions a high-molecular-weight shoulder begins to appear once conversion reaches 50% or more. The intensity of this high-molecular-weight shoulder increases at higher monomer conversion and the resultant polydispersity (PDI) increases slightly throughout the reaction. Considering both mechanisms for chain termination, the disproportionation produces unsaturated chain ends initially and then leads to the coupling of stars, while the radical combination results in direct star–star coupling. Conversely, samples prepared with a lower catalyst content or using a solvent of higher polarity result in products with narrower polydispersity and higher symmetry, with nearly monomodal GPC traces, as shown in Fig. 5 (obtained from Fig. 3(c)). A high concentration of catalyst tends to promote the formation of a relatively larger amount of high-molecular-weight species because of a greater degree of coupling between stars.

Fig. 6 shows the dependence of the molecular weight of the star polymers versus monomer conversion initiated by the AdPpBr **5** initiator. The drawn line represents the theoretical molecular weight, $M_{n(th)}$, calculated from:

$$M_{n(\mathrm{th})} = \Delta[\mathrm{M}]/[\mathrm{I}]_0 \times M_{\mathrm{W\ mon}} + M_{\mathrm{W\ init}} \quad (1)$$

We observe a near-linear increase in the measured number average molecular weight (M_n) versus monomer conversion up to ~85%, indicating that a living/controlled polymerization process proceeds in the polar media. The most probable explanation is that the polymerization has lower initiation efficiency due to its poor complex formation and poor control during polymerization in toluene. Consequently, not all of the four groups in each AdPpBr **5** molecule are activated, only a few propagating arms result or the star–star coupling forms. These results confirm that the initiator, AdPpBr **5**, is an efficient one for ATRP using the polar solvent anisole and a Cu complex as the activating agent.

The star polymers dissolved in 1,4-dioxane were hydrolyzed by NaOH, which cleaved them into free PMMA chains and adamantane cores. The molecular weights of the arms that were hydrolyzed by NaOH remain steadily constant with time, with the first 48 h of the reaction used as the standard time for this procedure. This observation—the steadily constant molecular weight with time—reveals that these arms are likely to be completely detached from the cores and that no PMMA hydrolysis within this time interval. Consistent with this analysis, Fig. 7 shows that the molecular weight of the PMMA star polymer decreases from 36,000 to 7500 after hydrolysis for 48 h. The experimental molecular weight of PMMA ($M_n = 7500\ \mathrm{g\ mol^{-1}}$) is in good agreement with the theoretical molecular weight ($M_n = 8000\ \mathrm{g\ mol^{-1}}$). PDI for these hydrolyzed PMMA arms is low (1.19), which suggests that these arms of the star PMMA are of uniform length and the initiation from AdPpBr **5** is highly efficient in high polar medium.

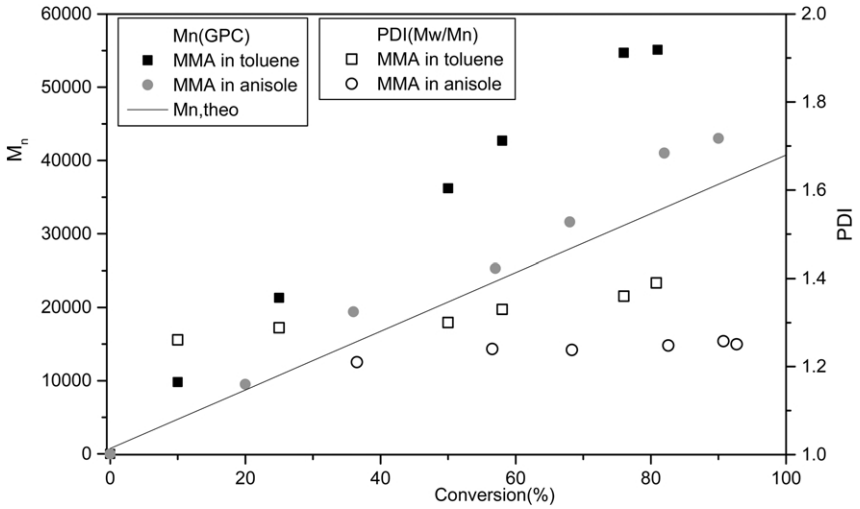

Fig. 6. The dependence of the molecular weights and polydispersity of the star polymers on the monomer conversion under different reaction conditions. The line represents the theoretical M_n.

4. Conclusions

We have demonstrated that a series of tetra-functionalized adamantane derivatives can be used as initiators for the ATRP on monomers of styrene and various acrylates. By properly adjusting the monomer-to-initiator ratio and the solvent polarity, we obtained a series of adamantane-containing star polymers covering a wide range of molecular weights. DSC measurements indicated that these star polymers have glass-transition temperatures similar to those of known high-molecular-weight linear polymers. The occurrence of star–star coupling, as a result of inevitable termination processes, leads to poor molecular polydispersity. AdPpBr is the most efficient initiator for the ATRP among the tetra-functionalized adamantane derivatives we studied. The phenylethyl halide derivative (AdPhCl) is a relatively poor initiator for the polymerization of MMA, with the rate of ATRP being significantly slower than that of AdPpBr. Furthermore, the rate of polymerization initiated by AdAcBr is the slowest among all the initiators investigated because of its lack of inductively or resonance-stabilizing substituents. Increasing the polarity of the solvent increases the solubility of the Cu(I)Br/ligand complex, and results in a homogeneous ATRP process. The star polymers can be hydrolyzed with NaOH to give the cleaved polymer chains with masses that are roughly a quarter those of the star polymers. The molecular weights of the arms released by the NaOH hydrolysis remained unchanged over time, even after reaction for 48 h (the length of time we used as a standard), which implies that these arms are likely to be completely released from the core structure and that no significant PMMA hydrolysis occurs thereafter.

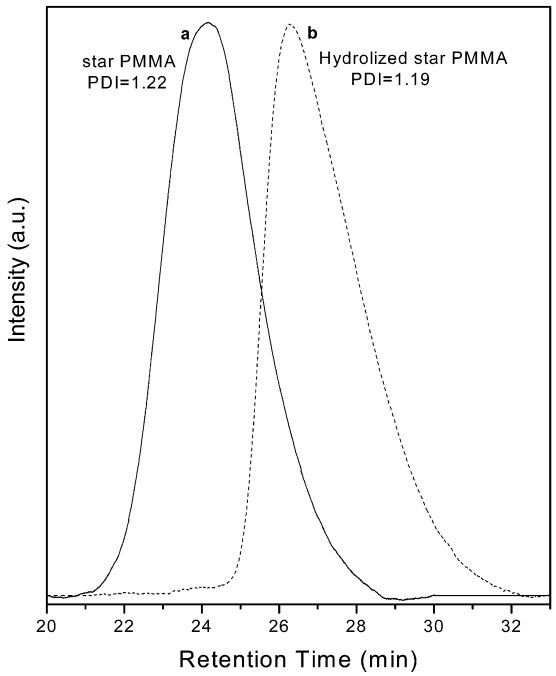

Fig. 7. GPC traces of a PMMA star polymer (a) before and (b) after hydrolysis.

Acknowledgements

This research was financially supported by the National Science Council, Taiwan, Republic of China, under Contract Nos. NSC-91-2216-E-009-018.

References

[1] Simms JA, Spinelli HJ. In: Hatada K, Kitayama T, Vogl O, editors. Macromolecular Design of Polymeric Materials. New York: Marcel Dekker; 1997. p. 379.
[2] For reviews of the properties of star polymers, see Bauer BJ, Fetters LJ. Rubber Chem Technol 1978;51:406.
[3] Bywater S. Adv Polym Sci 1979;30:90.
[4] Marsalko TM, Majoros I, Kennedy JP. Pure Appl Chem A 1997;34:775.

[5] Morton M, Helminiak TE, Gadkary SD, Bueche F. J Polym Sci 1962; 57:471.
[6] Shohi H, Sawamoto M, Higashimura T. Makromol Chem 1992;193: 2027.
[7] Sawamoto M. In: Matyjaszewski K, editor. Cationic polymerizations. New York: Marcel Dekker; 1996. p. 381.
[8] Kennedy JP, Jacob S. Acc Chem Res 1998;31:835.
[9] Cloutet E, Fillaut J, Astruc D, Gnanou Y. Macromolecules 1998;31: 6748.
[10] Quirk R, Tsai Y. Macromolecules 1998;31:8016.
[11] For reviews of the synthesis of star-shaped polymers by ionic living polymerization, see Morton M. Anionic polymerization: principle and practice. New York: Academic; 1983. p. 221.
[12] Hsieh HL, Quirk RP. Anionic polymerization. New York: Marcel Dekker; 1996. p. 333.
[13] Sawamoto M. In: Matyjaszewski K, editor. Cationic polymerization. New York: Marcel Dekker; 1996. p. 412.
[14] Sawamoto M, Kamigaito M. In: Ebdon JR, Eastmond GC, editors. New methods of polymer synthesis. Glasgow: Blackie; 1995. p. 37.
[15] Sawamoto M, Kanaoka S, Higashimura T. In: Sasabe H, editor. Hyper-structured molecules I: chemistry, physics and applications. Amsterdam: Gordon and Breach; 1999. p. 43.
[16] Hawker CJ. Acc Chem Res 1997;30:373.
[17] Hawker CJ, Mecerreyes D, Hedrick JL, Dubois Ph, Jerome R. Macromol Chem Phys 1997;298:155.
[18] Chong YK, Le TPT, Moad G, Rizzardo E, Thang SH. Macromolecules 1999;32:2071.
[19] Matyjaszewski K, Patten TE, Xia J. J Am Chem Soc 1997;119:674.
[20] Wang JS, Matyjaszewski K. J Am Chem Soc 1995;117:5614.
[21] Wang JS, Matyjaszewski K. Macromolecules 1995;28:7901.
[22] Kato M, Kamigaito M, Sawamoto M, Higashimura T. Macromolecules 1995;28:1721.
[23] Patten TE, Xia J, Abemathy T, Matyjaszewski K. Science 1996;272: 866.
[24] Perece V, Barbooiu B. Macromolecules 1995;28:7970.
[25] Haddleton DM, Jasieczek CB, Hannon MJ, Shooter AJ. Macromolecules 1997;30:2190.
[26] Granel C, Dubois P, Jerome R, Teyssie P. Macromolecules 1996;29: 8579.
[27] Uegaki H, Kotani Y, Kamigaito M, Sawamoto M. Macromolecules 1997;30:2249.
[28] Fredric MM, Vasily AM. J Org Chem 1999;64:8916.
[29] Vasily AM, Fredric MM. Langmuir 2001;17:1324.
[30] Raymond CFJ, Paul VRS. Chem Rev 1964;3:277.
[31] Davis KA, Matyjaszewski K. Macromolecules 2000;33:4039.
[32] Nanda AK, Matyjaszewski K. Macromolecules 2003;36:599.
[33] Wang JL, Grimaud T, Matyjaszewski K. Macromolecules 1997;30: 6507.
[34] Pattern TE, Matyjaszewski K. Adv Mater 1998;10:901.